

THE IMPORTANCE OF MODEL INSPECTION FOR BETTER UNDERSTANDING PERFORMANCE CHARACTERISTICS OF GRAPH NEURAL NETWORKS

Nairouz Shehata^{1,2}, Carolina Piçarra¹, Anees Kazi³, Ben Glocker¹

¹ Department of Computing, Imperial College London, UK

² Biomedical Engineering & Innovation Laboratory, Aswan Heart Centre, Egypt

³ Massachusetts General Hospital, Harvard University, USA

ABSTRACT

This study highlights the importance of conducting comprehensive model inspection as part of comparative performance analyses. Here, we investigate the effect of modelling choices on the feature learning characteristics of graph neural networks applied to a brain shape classification task. Specifically, we analyse the effect of using parameter-efficient, shared graph convolutional submodels compared to structure-specific, non-shared submodels. Further, we assess the effect of mesh registration as part of the data harmonisation pipeline. We find substantial differences in the feature embeddings at different layers of the models. Our results highlight that test accuracy alone is insufficient to identify important model characteristics such as encoded biases related to data source or potentially non-discriminative features learned in submodels. Our model inspection framework offers a valuable tool for practitioners to better understand performance characteristics of deep learning models in medical imaging.

Index Terms— Shape classification, graph neural networks, brain structures, 3D meshes, model inspection

1. INTRODUCTION

Understanding biological sex-based differences in brain anatomy provides valuable insights into both neurodevelopmental processes and cognitive functioning. Recent strides in the field of geometric deep learning [1], particularly the advent of Graph Neural Networks (GNNs), have revolutionised the analysis of complex, non-Euclidean data [2] to make predictions at a node, edge, or graph-level. This allows us to treat brain shapes as graphs, leveraging the power of GNNs to learn from complex structural anatomical data [3]. Discriminative feature embeddings can be withdrawn from these models, representing brain shapes as a continuous vector of numerical features that capture valuable structural and geometrical information for downstream prediction tasks [4]. Techniques like Principal Component Analysis (PCA) can be used to reduce the dimensionality of graph embeddings for visualisation, aiding the exploration of subgroup biases in the feature

space beyond the target label. This analysis may help practitioners ensure the reliability of their predictions, and is particularly important in applications where GNNs feature embeddings may be leveraged for new tasks, such as fine-tuning, domain transfer, or multi-modal approaches.

In this study, we dissect GNN models trained under different settings for the task of sex classification using 3D meshes of segmented brain structures. We inspect the learned feature embeddings at different layers within a multi-graph neural network architecture. Through this granular analysis, we reveal critical insights into the inner workings of our models, identifying important effects of different modelling choices. This research demonstrates the utility of conducting a model inspection framework as part of model development, highlighting insights that may guide practitioners in the selection of models with desired characteristics, avoiding biases, overfitting and better understanding the driving forces behind predictions.

2. METHODS

2.1. Imaging datasets

We used four neuroimaging datasets, including data from the UK Biobank imaging study (UKBB)¹ [5], the Cambridge Centre for Ageing and Neuroscience study (CamCAN) [6, 7], the IXI dataset², and OASIS3 [8]. Both UKBB and CamCAN brain MRI data were acquired with Siemens 3T scanners. The IXI dataset encompassed data collected from three clinical sites, each employing different scanning systems. CamCAN and IXI are acquired from healthy volunteers, while UKBB is an observational population study. The OASIS3 dataset consists of 716 subjects with normal cognitive function and 318 patients exhibiting varying stages of cognitive decline. For all four datasets, subjects with missing biological sex or age information were excluded. Data from UKBB was split into three sets, with 9,900 scans used for training, 1,099 for validation, and 2,750 for testing. CamCAN, IXI and OASIS3

¹Accessed under application 12579.

²<https://brain-development.org/ixi-dataset/>

were used as external test sets, with sample sizes of 652, 563, and 1,034, respectively.

The UKBB data is provided with a comprehensive pre-processing already applied, using FSL FIRST [9] to automatically segment 15 subcortical brain structures from T1-weighted brain MRI, including the brain stem, left/right thalamus, caudate, putamen, pallidum, hippocampus, amygdala, and accumbens-area. We apply our own pre-processing pipeline to the CamCAN, IXI, and OASIS3 datasets, closely resembling the UKBB pre-processing. Our pipeline includes skull stripping using ROBEX³ [10], bias field correction using N4ITK [11], and brain segmentation via FSL FIRST.

2.2. Graph representation

The anatomical brain structures are represented by meshes as an undirected graph composed of nodes, connected by edges forming triangular faces. The number of nodes for most structures is 642 and up to 1,068, whereas the number of edges per structure ranges between 3,840 and 6,396. The meshes are automatically generated by the FSL FIRST tool.

2.2.1. Node features

Each graph node can carry additional information, encoded as feature vectors. This can include spatial coordinates or more complex geometric descriptors. While computer vision has transitioned from hand-crafted features to end-to-end deep learning, we have previously demonstrated the value of using geometric feature descriptors in GNN-based shape classification [12]. We employ Fast Point Feature Histograms (FPFH) [13], a pose invariant feature descriptor shown to substantially boost classification performance. To compute FPFH features on a mesh, a point feature histogram is first generated, involving the selection of neighboring points within a defined radius around each query point. The Darboux frame is subsequently defined, and angular variations are computed. This process involves several steps, including the estimation of normals and the calculation of angular variations, resulting in a vector of 33 features at each node.

2.2.2. Mesh registration

Mesh registration is an optional pre-processing step, with the goal to remove spatial variability across subjects and datasets. Here, we investigate the use of rigid registration aligning all meshes for a specific brain structure to a standardised orientation using the closed-form Umeyama approach [14]. This method employs a singular value decomposition-based optimisation to obtain an optimal rigid transformation between two given meshes. For each of the 15 brain structures, we select a reference mesh from a random subject from the UKBB dataset, and align the meshes from all other

³<https://www.nitrc.org/projects/robex>

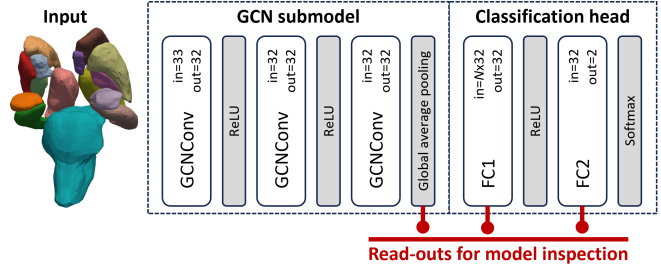


Fig. 1: Model architecture consisting of a graph convolutional network (GCN) submodel feeding graph embeddings into a classification head with two fully connected layers (FC1 and FC2). Where N is the number of brain substructures, 15. For our model inspection, we read out the feature vectors from the GCN submodel, FC1, and FC2.

subjects to this reference. As a result, shape variability due to orientation and position differences is minimised and the remaining variability is expected to primarily represent anatomical differences across subjects.

2.3. Multi-graph neural network architecture

Our general GNN architecture is comprised of two main components; the *GCN submodel* which aims to learn graph embeddings over 3D meshes using multiple graph convolutional layers [12] and an *MLP classification head* that takes the graph embeddings as inputs and performs the final classification using two fully connected layers (cf. Fig. 1).

The input to our models are 15 subgraphs representing 15 brain structures, extracted from T1-weighted brain scans. We consider two approaches for learning graph embeddings with GCN submodels. The first approach, referred to as *shared submodel*, uses a single GCN submodel that learns from all 15 subgraphs. Here, the weights of the graph convolutional layers are shared across brain structures. The shared submodel approach is parameter-efficient and aims to learn generic shape features. For the second approach, referred to as *non-shared submodel*, each subgraph is fed into a structure-specific GCN submodel. The non-shared submodel approach has more parameters and may capture structure-specific shape features. In both approaches, the architecture of the GCN submodel is identical and consists of three graph convolutional layers [15] with Rectified Linear Unit (ReLU) activations. A global average pooling layer is used as a readout layer, aggregating node representations into a single graph-level feature embedding. The embeddings from individual structures are stacked to form a subject-level feature embedding which is passed to the classification head.

2.4. Model inspection

Our model inspection approach is focused on evaluating the separability of the target label (biological sex, Male and

Female) and data source classes (UKBB, CamCAN, IXI or OASIS3) through feature inspection. Each test set sample is passed through the complete pipeline and its feature embeddings are saved at three different stages: at the output layer of the GCN submodel and at the first (FC1) and second (FC2) fully connected layers of the classification head. The dimensions of these embeddings are, respectively, 480 (15 substructures times the hidden layer size, 32), 32 and 2. To allow for visual inspection, the feature embeddings from the GCN and FC1 layers are inputted to a PCA model to reduce their dimensionality. The PCA modes capture the directions of the largest variation in the high-dimensional feature space, allowing us to visualise feature separation in 2D scatter plots. We randomly sample 500 subjects from each dataset for the visualisations. Given that all the models were trained to classify biological sex, a clear separation should be expected between the Male and Female classes in the first PCA modes.

3. EXPERIMENTS & RESULTS

For a thorough evaluation, we trained and tested the four models - shared and non-shared GCN submodels, and with and without mesh rigid registration - on identical data splits. All code was developed using PyTorch Geometric and PyTorch Lightning for model implementation and data handling. We used the Adam optimiser [16] with a learning rate of 0.001, and employed the standard cross entropy loss for classification. Random node translation was used as a data augmentation strategy with a maximum offset of 0.1mm [17]. This was shown to improve performance in our previous study [12]. Model selection was done based on the loss of the validation set. Our code is made publicly available⁴.

3.1. Classification performance

Figure 2 summarises the classification performance of the four models, showing the ROC curves together with the area under the curve (AUC) metric, reported separately for each of the four test datasets. There are two main observations: (i) There are very little differences in the absolute performance across the four models. Comparing the *shared* vs *non-shared* submodel, the AUC performance is comparable. When comparing models *with* and *without* mesh registration, we find the generalisation gap decreases between in-distribution test (UKBB) and the external test data (CamCAN, IXI, OASIS3). However, we also observe a small drop in performance on the in-distribution test data when using mesh registration, compared to not using registration. A practitioner using internal test results for final model selection may opt for using a *shared* submodel, due to its parameter efficiency, *without* mesh registration, due to convenience. As we will see next, this choice may be suboptimal as test accuracy alone is insufficient to identify important model characteristics.

⁴<https://github.com/biomed-mira/medmesh>

3.2. Effect of using structure-specific submodels

For the models that use a *shared* submodel, we observe that the GCN feature embeddings are non-discriminative with respect to the target label. Separation seems completely missing in the *shared* model *without* registration (see Fig. 3a), with only weak separation in the *shared* model *with* registration (see Fig. 3c). For these models, the classification heads will primarily contribute to the model performance. For the models with a *non-shared* submodel, we find a much better separability for the GCN features *with* and *without* mesh registration (cf. Figs. 3b, d). Here, the GCN features will meaningfully contribute to the models' classification performance.

3.3. Effect of mesh registration

When studying the effect of mesh registration, we can clearly observe that *without* registration, the GCN feature embeddings from the submodel strongly encode data source, showing separate clusters for UKBB and external test data (cf. Figs. 3a,b). When introducing mesh registration as a pre-processing step, we note a significant improvement, with an almost entirely removed separation of datasets in the GCN layer independent of whether a *shared* and *non-shared* submodel is used (Figs. 3c, d). The separability of the target label in the GCN layer is well defined for the *non-shared* submodel (Fig. 3d), while remaining weak for the *shared* submodel (Fig. 3c). Rigid registration as a pre-processing step seems to not only improve the learning efficiency of the GCN submodel, but also its ability to generalise across data distributions.

4. CONCLUSION

Our findings underscore the limitations of relying solely on test accuracy for model selection, particularly when focusing on in-distribution test accuracy. We demonstrate that this may lead practitioners to select models with undesired characteristics where GCN features are non-discriminative for the prediction task and/or strongly encode biases such as data source. Using a comprehensive model inspection, we were able to identify variations in the model characteristics and better understand what drives the final prediction (GCN submodel vs classification head). The importance of this becomes evident when considering applications such as fine-tuning, domain transfer, or multi-modal approaches, where GCN feature embeddings may be leveraged for new tasks.

Our model inspection framework can be easily applied to other models, tasks, and purposes. It was previously used to detect biases in chest radiography disease detection models [18]. Here, we strongly advocate for the wider use of model inspection as an integral part of comparative performance analyses. We hope that our work can contribute to improving the reliability of model selection in all areas of deep learning for biomedical image analysis.

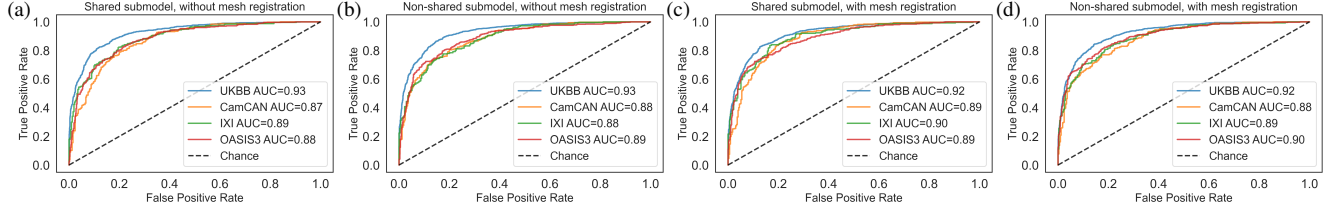


Fig. 2: Sex classification performance for four models; **(a)** *shared* and **(b)** *non-shared* submodel *without* mesh registration, **(c)** *shared* and **(d)** *non-shared* submodel *with* mesh registration. We observe that the generalisation gap between the in-distribution test data (UKBB) and the external test data (CamCAN, IXI, OASIS3) closes *with* mesh registration. Overall, there are only small differences in performance, illustrating that test accuracy alone is insufficient to identify variations in model characteristics.

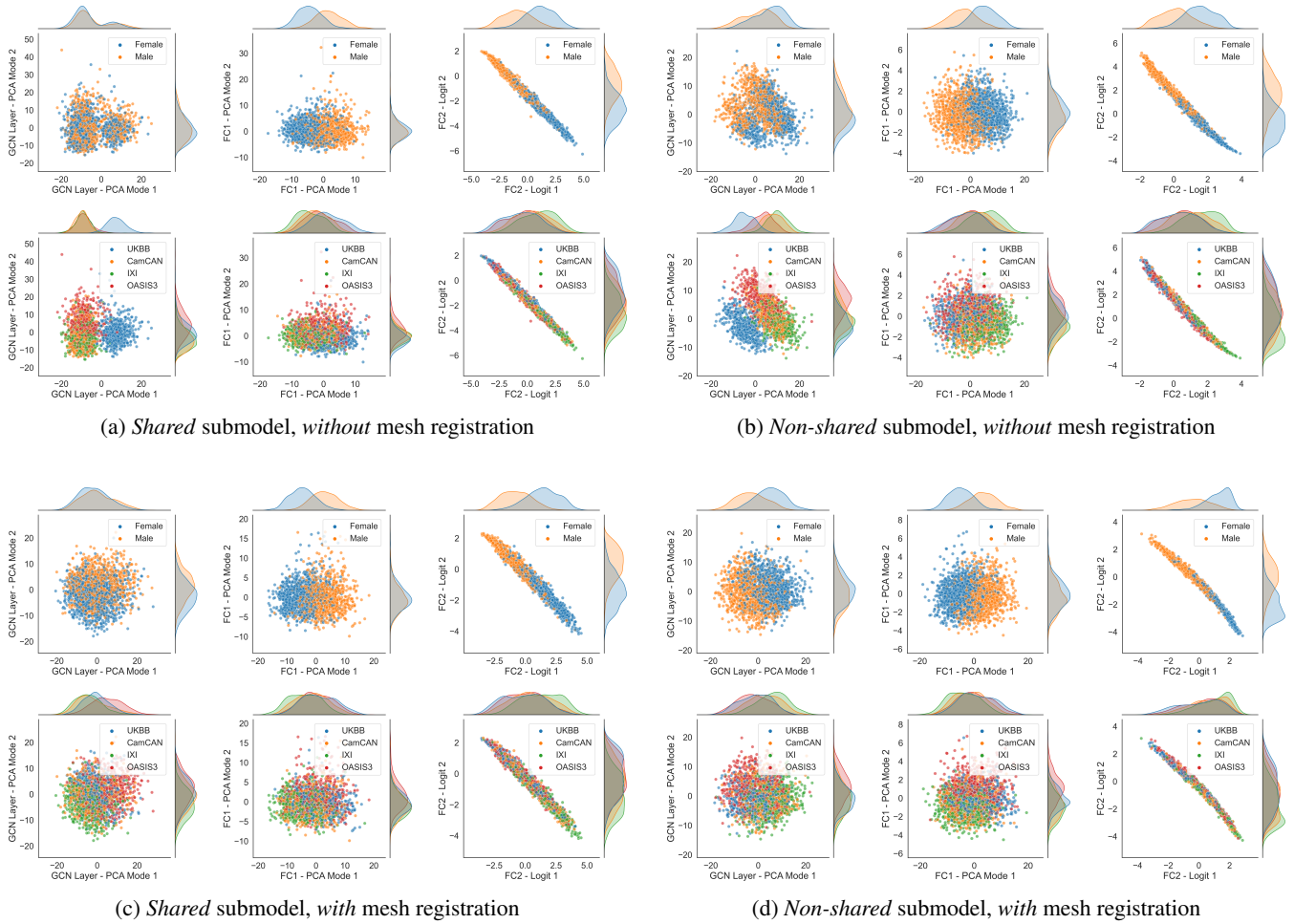


Fig. 3: Effect of modelling choices on feature separability for four different models at their the GCN layer (left), first fully connected layer FC1 (middle), and output layer FC2 (right). **Models:** **(a,c)** *shared* and **(b,d)** *non-shared* GCN submodel, and **(a,b)** *without* and **(c,d)** *with* mesh registration. For each model, we show the separation by target label in the top row, and the separation by dataset in the bottom row. **Effect of submodel:** The models in **(a,c)** with a *shared* submodel are unable to learn discriminative GCN features for the prediction task, while the models in **(b,d)** with a *non-shared* submodel show much better task-related separability in the GCN features. **Effect of registration:** The models models in **(a,b)** *without* registration strongly encode information about the data source in the GCN layer. This is much reduced for the models in **(c,d)** *with* mesh registration.

5. ACKNOWLEDGMENTS

Nairouz Shehata is grateful for the support by the Magdi Yacoub Heart Foundation and Al Alfi Foundation.

6. COMPLIANCE WITH ETHICAL STANDARDS

This study uses secondary, fully anonymised data which is publicly available and is exempt from ethical approval.

7. REFERENCES

- [1] Michael M Bronstein, Joan Bruna, Yann LeCun, Arthur Szlam, and Pierre Vandergheynst, “Geometric deep learning: going beyond euclidean data,” *IEEE Signal Processing Magazine*, vol. 34, no. 4, pp. 18–42, 2017.
- [2] Zonghan Wu, Shirui Pan, Fengwen Chen, Guodong Long, Chengqi Zhang, and S Yu Philip, “A comprehensive survey on graph neural networks,” *IEEE transactions on neural networks and learning systems*, vol. 32, no. 1, pp. 4–24, 2020.
- [3] Ignacio Sarasua, Sebastian Pölsterl, and Christian Wachinger, “Hippocampal representations for deep learning on alzheimer’s disease,” *Scientific reports*, vol. 12, no. 1, pp. 1–13, 2022.
- [4] Alaa Bessadok, Mohamed Ali Mahjoub, and Islem Rekek, “Graph neural networks in network neuroscience,” *IEEE Transactions on Pattern Analysis and Machine Intelligence*, vol. 45, no. 5, pp. 5833–5848, 2022.
- [5] Cathie Sudlow, John Gallacher, Naomi Allen, Valerie Beral, Paul Burton, John Danesh, Paul Downey, Paul Elliott, Jane Green, Martin Landray, et al., “UK Biobank: an open access resource for identifying the causes of a wide range of complex diseases of middle and old age,” *PLoS medicine*, vol. 12, no. 3, pp. e1001779, 2015.
- [6] Jason R. Taylor, Nitin Williams, Rhodri Cusack, Tibor Auer, Meredith A. Shafto, Marie Dixon, Lorraine K. Tyler, Richard N. Henson, et al., “The Cambridge Centre for Ageing and Neuroscience (Cam-CAN) data repository: structural and functional MRI, MEG, and cognitive data from a cross-sectional adult lifespan sample,” *NeuroImage*, vol. 144, pp. 262–269, 2017.
- [7] Meredith A. Shafto, Lorraine K. Tyler, Marie Dixon, Jason R. Taylor, James B. Rowe, Rhodri Cusack, Andrew J. Calder, William D. Marslen-Wilson, John Duncan, Tim Dalgleish, et al., “The Cambridge Centre for Ageing and Neuroscience (Cam-CAN) study protocol: a cross-sectional, lifespan, multidisciplinary examination of healthy cognitive ageing,” *BMC Neurology*, vol. 14, no. 1, pp. 204, 2014.
- [8] Pamela J LaMontagne, Tammie LS Benzinger, John C Morris, Sarah Keefe, Russ Hornbeck, Chengjie Xiong, Elizabeth Grant, Jason Hassenstab, Krista Moulder, Andrei G Vlassenko, et al., “Oasis-3: longitudinal neuroimaging, clinical, and cognitive dataset for normal aging and alzheimer disease,” *MedRxiv*, pp. 2019–12, 2019.
- [9] Brian Patenaude, Stephen M Smith, David N Kennedy, and Mark Jenkinson, “A bayesian model of shape and appearance for subcortical brain segmentation,” *Neuroimage*, vol. 56, no. 3, pp. 907–922, 2011.
- [10] Juan Eugenio Iglesias, Cheng-Yi Liu, Paul M Thompson, and Zhuowen Tu, “Robust brain extraction across datasets and comparison with publicly available methods,” *IEEE Transactions on Medical Imaging*, vol. 30, no. 9, pp. 1617–1634, 2011.
- [11] Nicholas J Tustison, Brian B Avants, Philip A Cook, Yuanjie Zheng, Alexander Egan, Paul A Yushkevich, and James C Gee, “N4ITK: improved N3 bias correction,” *IEEE Transactions on Medical Imaging*, vol. 29, no. 6, pp. 1310–1320, 2010.
- [12] Nairouz Shehata, Wulfie Bain, and Ben Glocker, “A comparative study of graph neural networks for shape classification in neuroimaging,” in *Geometric Deep Learning in Medical Image Analysis*. PMLR, 2022, pp. 160–171.
- [13] Radu Bogdan Rusu, Nico Blodow, and Michael Beetz, “Fast point feature histograms (fpfh) for 3d registration,” in *2009 IEEE international conference on robotics and automation*. IEEE, 2009, pp. 3212–3217.
- [14] Shinji Umeyama, “Least-squares estimation of transformation parameters between two point patterns,” *IEEE Transactions on Pattern Analysis & Machine Intelligence*, vol. 13, no. 04, pp. 376–380, 1991.
- [15] Thomas N Kipf and Max Welling, “Semi-supervised classification with graph convolutional networks,” *arXiv preprint arXiv:1609.02907*, 2016.
- [16] Diederik P Kingma and Jimmy Ba, “Adam: A method for stochastic optimization,” *arXiv preprint arXiv:1412.6980*, 2014.
- [17] Jiajun Zhou, Jie Shen, and Qi Xuan, “Data augmentation for graph classification,” in *Proceedings of the 29th ACM International Conference on Information & Knowledge Management*, 2020, pp. 2341–2344.
- [18] Ben Glocker, Charles Jones, Mélanie Roschewitz, and Stefan Winzeck, “Risk of bias in chest radiography deep learning foundation models,” *Radiology: Artificial Intelligence*, vol. 5, no. 6, pp. e230060, 2023.